

Sonocatalytic ozonation, with nano-TiO₂ as catalyst, for degradation of 4-chloronitrobenzene in aqueous solution

Behrouz Vahid · Tayebeh Mousanejad ·
Alireza Khataee

Received: 14 July 2014 / Accepted: 21 August 2014 / Published online: 7 September 2014
© Springer Science+Business Media Dordrecht 2014

Abstract The results for the degradation efficiency of 4-chloronitrobenzene (4-CNB) by various advanced oxidation processes in a batch mode using nano-structured titanium dioxide demonstrated the order of $O_3/US/TiO_2 > US/O_3 > O_3/TiO_2 > O_3 > US/TiO_2 > US$. The utilized TiO₂ nanoparticles were characterized by X-ray diffraction (XRD) and transmission electron microscopy (TEM). Moreover, all processes obeyed pseudo-first order kinetics. Then, the effect of the main operational conditions including pH, ozone, initial 4-CNB concentration, TiO₂ dosage and ultrasonic power on 4-CNB degradation was studied in the coupled $O_3/US/TiO_2$ process as the most significant treatment method with a high synergistic effect. The optimal pH and TiO₂ dosage were selected to be 9 and 50 mg/L owing to the efficient indirect attack of hydroxyl radicals and less screening effects of TiO₂ particles on ultrasonic waves, respectively. By increasing the amount of O₃ concentration and ultrasonic power, the degradation of 4-CNB was enhanced due to the more production of reactive oxygen species. However, the opposite trend was observed for 4-CNB concentration because the same amounts of generated oxidizing species under the identical experimental conditions had to degrade more organic pollutants and its degradation intermediates. Eventually, the total organic carbon (TOC) was utilized to monitor the mineralization of 4-CNB in the above-mentioned processes and the same results were obtained with lower rate constants compared to degradation rate constants.

B. Vahid (✉)

Department of Chemical Engineering, College of Engineering, Tabriz Branch, Islamic Azad University, Tabriz, Iran
e-mail: behrouz.vahid@gmail.com; behrouz_vahid@iaut.ac.ir

T. Mousanejad

Department of Chemistry, College of Science, Khoy Branch, Islamic Azad University, Khoy, Iran

A. Khataee

Research Laboratory of Advanced Water and Wastewater Treatment Processes, Department of Applied Chemistry, Faculty of Chemistry, University of Tabriz, Tabriz, Iran

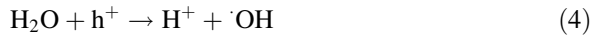
Keywords Sonocatalytic ozonation · Nano-TiO₂ · 4-Chloronitrobenzene · Degradation · Mineralization

Introduction

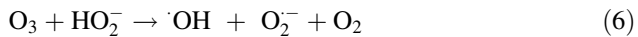
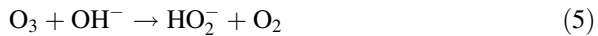
Large amounts of 4-chloronitrobenzene (4-CNB) are widely used as a major chemical intermediate in the industrial preparation of such diverse products as dyes, pesticides, pharmaceuticals, corrosion inhibitors, and gasoline additives. Substantial amounts of 4-CNB are released into the aquatic environment, owing to its solubility and stability during production and use [1]. It is regarded as a persistent organic pollutant (POP) and the US Environmental Protection Agency (EPA) has classified it as a priority pollutant because of its high toxicity and carcinogenic potential. Hence, governments, for example that of China, limit the maximum concentration of 4-CNB in drinking and surface water to 50 and 500 µg/L, respectively [2]. Consequently, its removal from water is essential from an environmental perspective. 4-CNB is bioresistant and, as a result, conventional methods of treatment are not effective. Because physicochemical processes, for example adsorption and coagulation generate secondary phases without solving the basic problem [3], advanced oxidation processes (AOPs), for example use of ozone (O₃) [4], ultrasound (US) [5], US/TiO₂ [6], and O₃/UV/TiO₂ [7], are convenient not only for oxidation and degradation of 4-CNB but also for its complete mineralization and production of no secondary waste. Reactive oxygen species (ROS), particularly hydroxyl radicals ([•]OH) are of crucial importance in the use of AOPs because of their unselective reaction with organic compounds and their conversion of these to water, carbon dioxide, and inorganic mineral salts [8].

The source of sonochemical effects is cavitation, i.e. the generation of tiny bubbles, when negative acoustic pressure is sufficient to separate water molecules in the rarefaction cycle of an ultrasonic wave, and the positive acoustic pressure during the compression cycle. A cavitation bubble can be regarded as a micro reactor growing for a few cycles then eventually collapsing, generating high pressures and temperatures which cause decomposition of water to hydroxyl radicals (Eq. 1) [9]. Although the US process is safe, clean, and efficient, the rate of degradation is rather slow, so coupled techniques are usually used to enhance the efficiency of degradation as a result of synergistic effects [10]. For example, when such semiconductors as TiO₂ are used with ultrasonic irradiation as energy source, electron–hole pairs are generated in conduction and valence bands, respectively (Eq. 2) [11]. These can then react with electron donors or acceptors to produce ROS-like hydroxyl or superoxide radicals (Eqs. 3, 4) [12, 13]. Moreover, more cavitation bubbles can be produced in the presence of solid particles owing to the lower tensile strength of the solid–liquid interface and the greater number of cavitation nuclei in their crevices [14].

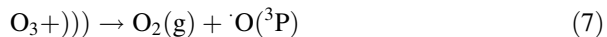




Ozone, because of its high reactivity and strongly oxidizing properties ($E^0 = 2.07 \text{ V}$), make it an appropriate disinfectant for application in water-treatment processes. Under basic conditions O_3 decomposes rapidly, yielding $\cdot\text{OH}$ radicals (Eqs. 5, 6), leading to degradation of organic pollutants; O_3 also degrades organic pollutants by its electrophilic reaction under acidic conditions [15]. It has, however, been recognized that degradation of contaminants may not be complete in conventional O_3 treatment [16].



TiO_2 -catalyzed ozonation (O_3/TiO_2) is more efficient than use of O_3 alone for degradation of such organic pollutants as oxalic and humic acids. This can be attributed to dissolution and decomposition of more ozone in the presence of TiO_2 , owing to reaction of ozone with hydroxyl groups present on the TiO_2 surface in water [17]. In addition, combination of US irradiation with O_3 (US/ O_3) is another combined treatment method used to oxidize the wide variety of POPs in aqueous solution [18]. This is explained on the basis of the mechanical effects of ultrasound and reduction of the mass transfer limitation of O_3 from the gas phase to the bulk solution; hence, more active radicals can be generated by these reactions (Eqs. 7, 8) [19].



To the best of our knowledge, there is no report on the degradation of 4-CNB, as organic pollutant, by use of coupled $\text{O}_3/\text{US}/\text{TiO}_2$, which can be regarded as a convenient and clean method of treatment for enhancing degradation and mineralization efficiency. In this study, first, the efficiency and kinetics of degradation of 4-CNB by US, US/TiO_2 , O_3 , O_3/TiO_2 , US/O_3 , and $\text{O}_3/\text{US}/\text{TiO}_2$ were compared to discover synergistic effects. The effect of the initial concentrations of 4-CNB and ozone, initial pH, US power, and amount of catalyst on the degradation and mineralization of the pollutant in the coupled $\text{O}_3/\text{US}/\text{TiO}_2$ process was then investigated.

Experimental

Materials and characterization of TiO_2 nanoparticles

Titanium dioxide nanoparticles (Degussa P25, Germany) of average size 21 nm and surface area $50 \pm 15 \text{ m}^2/\text{g}$, containing 80 % anatase and 20 % rutile phases, were used as the semiconductor catalyst. X-ray diffraction (XRD; D5000; Siemens, Germany) and transmission electron microscopy (TEM; JEM-2200FS; Jeol, Japan)

were used to confirm the nano-crystalline structure of the TiO_2 . The main diffraction peaks in the XRD patterns (Fig. 1a), at approximately $2\theta = 25^\circ$ and 27° , originated from the anatase and rutile phases, respectively [20]. Moreover, as can be seen from the TEM image (Fig. 1b), the size of the TiO_2 nanoparticles was approximately 20 nm, consistent with the known mean crystal size.

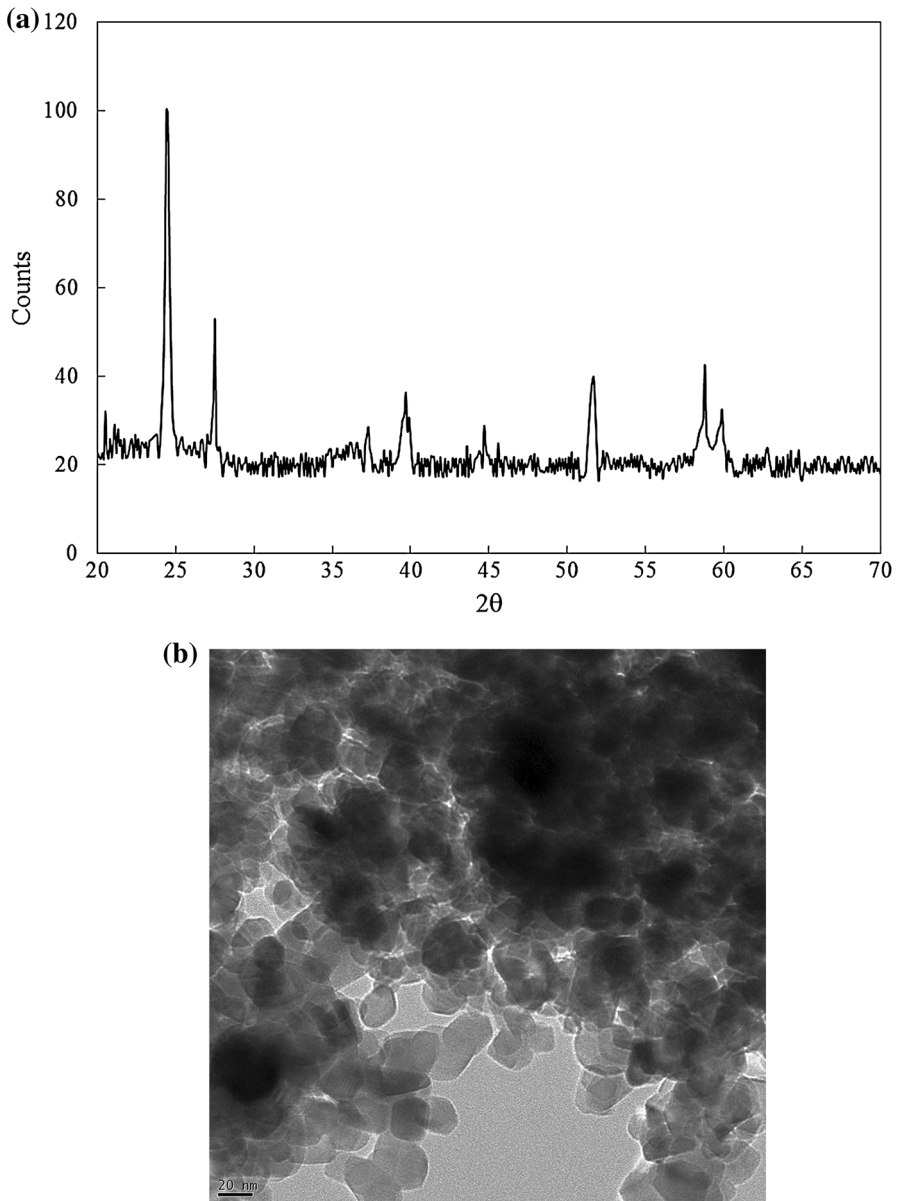


Fig. 1 a XRD pattern and b TEM image of the TiO_2 nanoparticles

Other chemicals were obtained from Merck (Germany) and used without further purification.

Experimental set-up and procedure

Experiments were performed in batch mode in a cylindrical quartz reactor of inner diameter 8 cm and total volume 500 mL. The ultrasonic processor (UP 400S; Hielscher, Germany) had variable power control (80, 240, and 400 W) and was equipped with a 24-kHz convertor and a pure titanium probe tip of diameter 14 mm and height 100 mm. A calorimetric method was used to determine the amount of ultrasonic power entering the solution (Eq. 9):

$$\text{Power} = (dT/dt) C_p M \quad (9)$$

where C_p and M are the heat capacity ($\text{J kg}^{-1} \text{K}^{-1}$) and mass of water (kg), respectively. Temperature (T) was plotted against time (t), and (dT/dt) was estimated from the plot. Actual power dissipation in the solution was measured as 0.09, 0.25, and 0.4 W/mL for US power of 80, 240, and 400 W, respectively [5]. The glass cylinder was sealed by a polyethylene cap during operation, and the US probe fixed at the center of the cap was then immersed in the solution. Ozone, provided from an ozone generator (Donali, Iran), was fed into the reactor from the bottom by use of a diffuser; its concentration was adjusted by changing the voltage and determined by use of the potassium iodide (KI) method [15]. In each experiment, 250 mL reaction mixture containing a known amounts of 4-CNB and TiO_2 was prepared. Sodium hydroxide or perchloric acid was used for adjustment of the pH of the solution. The solution was treated by use of a known amount of O_3 at a known US power. A temperature-controlled bath was used to maintain the temperature at 25 °C. Samples were withdrawn by use of a glass syringe after specific reaction times, and centrifuged and filtered for separation of TiO_2 particles (if present). The samples were then analyzed to determine the amount of 4-CNB degraded.

Analytical methods

High-performance liquid chromatography (HPLC; SCL-6A; Shimadzu, Japan) was used to determine the concentration of 4-CNB (C) in the solution. A Zorbax column (5 μm , C18) with methanol–water 8:2 (v/v) as mobile phase, at a flow rate of 1.0 mL/min, were used for HPLC analysis. To monitor the mineralization of 4-CNB, total organic carbon (TOC) was measured by catalytic oxidation (TOC-5000; Shimadzu, Japan).

Results and discussion

Comparison of different processes for degradation of 4-CNB, and study of the kinetics

Degradation efficiency (DE%) was defined as the ratio of the amount of 4-CNB degraded ($C_0 - C$) at a specific time to the initial concentration (C_0), as a percentage.

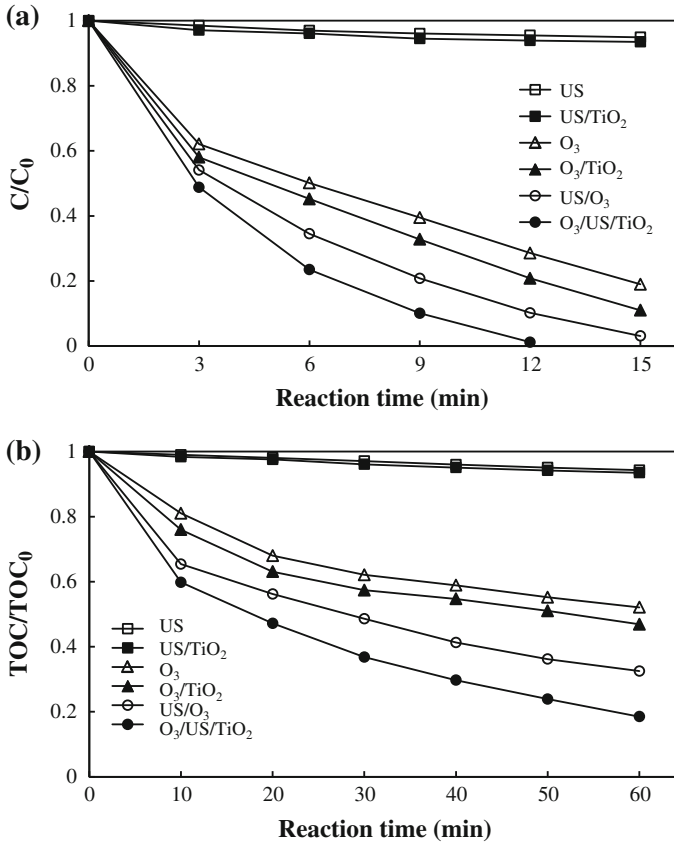


Fig. 2 Degradation (a) and mineralization (b) curves for decomposition of 4-CNB by use of different oxidation processes. Experimental conditions: $C_0 = 40$ mg/L, pH = 9, O_3 concentration = 5.8 mg/L, US power = 400 W, and amount of $TiO_2 = 50$ mg/L

The synergistic effect in AOPs was defined as interaction between two or more processes that generates an effect more than the sum of the individual effects [21]. The order of increasing DE % for 4-CNB (40 mg/L) for a variety of AOPs after treatment for 12 min was US (4.5 %), US/TiO₂ (6.1 %), O₃ (71.4 %), O₃/TiO₂ (79.18 %), US/O₃ (89.8 %), and O₃/US/TiO₂ (98.8 %) (Fig. 2a).

The results revealed that combined heterogeneous sonication and ozonation with high oxidative capability was an effective process for degradation of 4-CNB. These observations can be simply interpreted on the basis of production of extra ROS, especially hydroxyl radicals, owing to the synergistic effects of four processes:

- 1 generation of electron-hole pairs in TiO₂ by sonication (Eq. 2) [22];
- 2 increased dissolution of O₃ in the presence of TiO₂ [17] and US [23];
- 3 action of O₃ as an electron acceptor, preventing electron-hole recombination (Eqs. 10–12) [24]; and

Table 1 Pseudo-first-order degradation and mineralization rate constants for 4-CNB in the different treatment processes

Treatment process	Degradation rate constant (min^{-1})	Correlation coefficient (R^2)	Mineralization rate constant (min^{-1})	Correlation coefficient (R^2)
US	0.003	0.960	0.001	0.998
US/TiO ₂	0.004	0.914	0.001	0.988
O ₃	0.103	0.986	0.010	0.918
O ₃ /TiO ₂	0.137	0.980	0.011	0.910
US/O ₃	0.217	0.966	0.017	0.946
O ₃ /US/TiO ₂	0.347	0.931	0.026	0.977

[4-CNB]₀ = 40 mg/L, pH = 9, O₃ concentration = 5.8 mg/L, US power = 400 W, and amount of TiO₂ = 50 mg/L

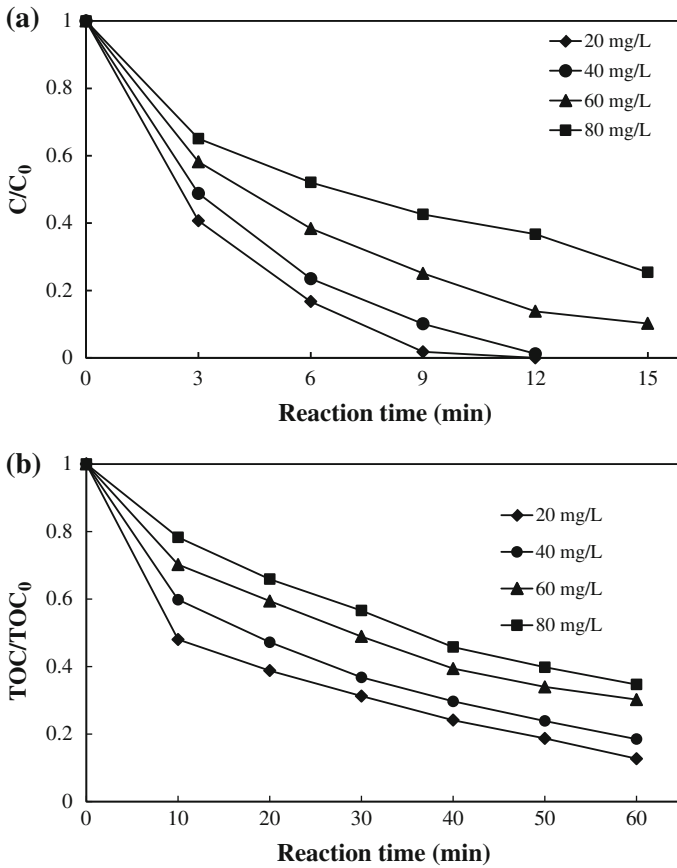


Fig. 3 Effect of initial 4-CNB concentration on the **a** degradation and **b** mineralization of 4-CNB by the O₃/US/TiO₂ process. Experimental conditions: pH = 9, O₃ concentration = 5.8 mg/L, US power = 400 W, and amount of TiO₂ = 50 mg/L

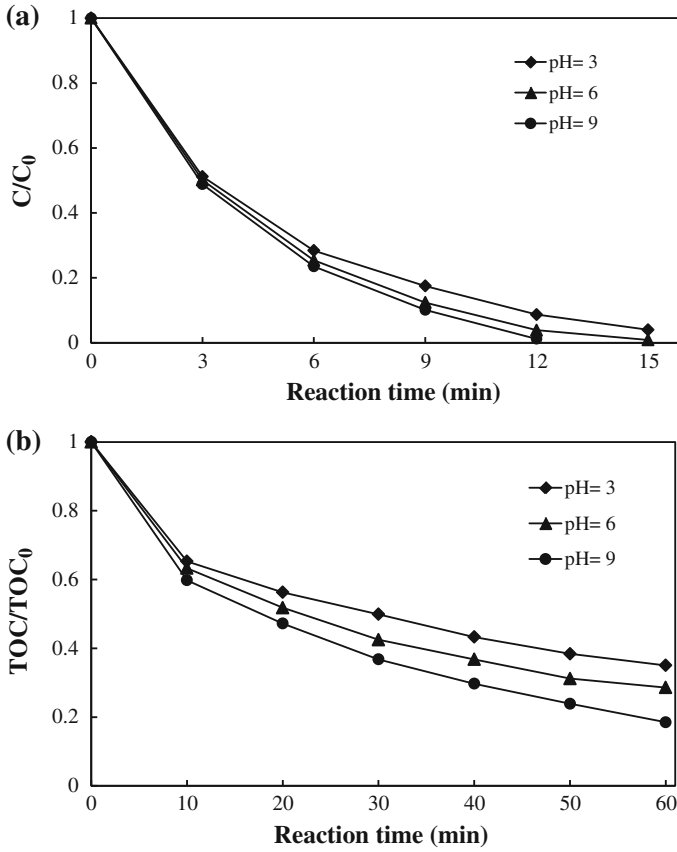
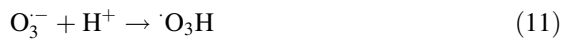


Fig. 4 Effect of pH on the **a** degradation and **b** mineralization of 4-CNB by the O₃/US/TiO₂ process. Experimental conditions: C₀ = 40 mg/L, O₃ concentration = 5.8 mg/L, US power = 400 W, and amount of TiO₂ = 50 mg/L

- 4 sonoluminescence, as a result of generation of a small amount of light by semiconductor particles (in the absence of UV irradiation) which activates O₃ [24] and TiO₂ [14] (Eqs. 13, 14).



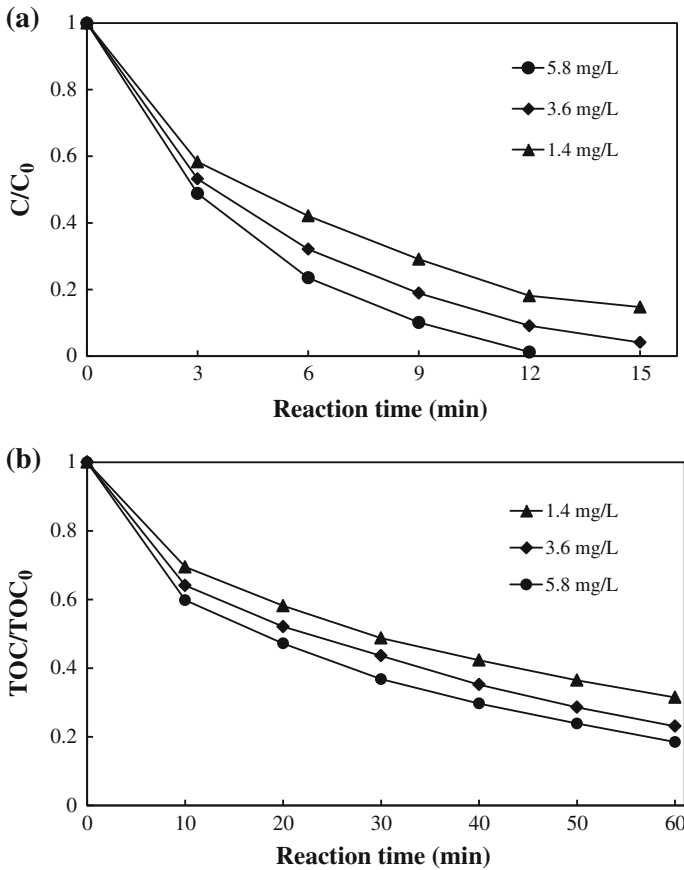


Fig. 5 Effect of ozone concentration on the **a** degradation and **b** mineralization of 4-CNB by the O₃/US/TiO₂ process. Experimental conditions: C₀ = 40 mg/L, pH = 9, US power = 400 W, and amount of TiO₂ = 50 mg/L



All the AOPs used in this investigation obeyed pseudo-first-order kinetics (Eq. 15), consistent with results from other, similar, studies [6, 15, 25, 26]:

$$(-dC/dt) = k_{app} \times C \tag{15}$$

The apparent pseudo-first-order rate constants (*k_{app}*) for degradation of 4-CNB by use of these processes were calculated from the slopes of plots of ln (C/C₀) against time (*t*); the results are listed in Table 1. For all the plots, straight lines with correlation coefficients (*R*²) >0.90 verified the proposed first-order kinetics. The synergistic effect of O₃ and US/TiO₂ was significant for 4-CNB degradation. It was determined as 0.69 from the degradation rate constants, by use of the equation [27]:

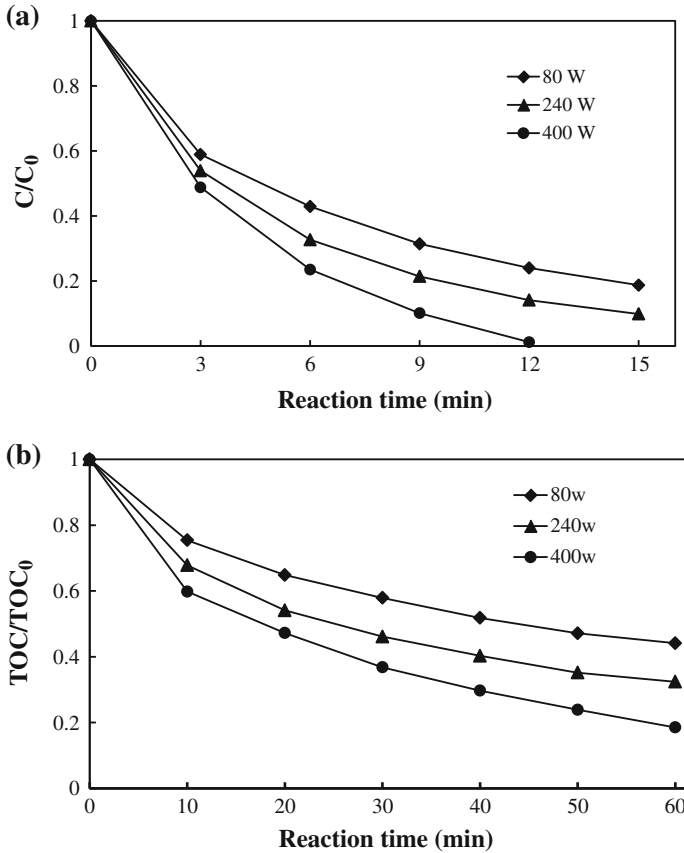


Fig. 6 Effect of US power on the **a** degradation and **b** mineralization of 4-CNB by the O₃/US/TiO₂ process. Experimental conditions: C₀ = 40 mg/L, pH = 9, O₃ concentration = 5.8 mg/L, and amount of TiO₂ = 50 mg/L

$$\text{Synergy} = (k_{\text{O}_3/\text{US}/\text{TiO}_2} - (k_{\text{O}_3} + k_{\text{US}/\text{TiO}_2}))/k_{\text{O}_3/\text{US}/\text{TiO}_2} \quad (16)$$

Furthermore, the same order of efficiency (US (5.7 %), US/TiO₂ (6.5 %), O₃ (47.9 %), O₃/TiO₂ (53.1 %), US/O₃ (67.5 %) and O₃/US/TiO₂ (81.5 %)) and kinetics were observed for mineralization of 4-CNB by the above-mentioned AOPs, as monitored by TOC removal after treatment for 60 min (Fig. 2b). The apparent pseudo-first-order rate constants (k_{app}) for mineralization of 4-CNB were determined by the same method, as explained above; the results are listed in Table 1 [28]. The synergistic effect of O₃ and US/TiO₂ was also remarkable for 4-CNB mineralization and was calculated from the mineralization rate constants (Eq. 16) to be 0.57. Comparison of the data in Table 1 reveals that the rate of mineralization was lower than the rate of degradation in an AOP under identical operating conditions, owing to the need to degrade the intermediates formed to water, carbon dioxide, and inorganic salts during these processes [28]. Consequently, other

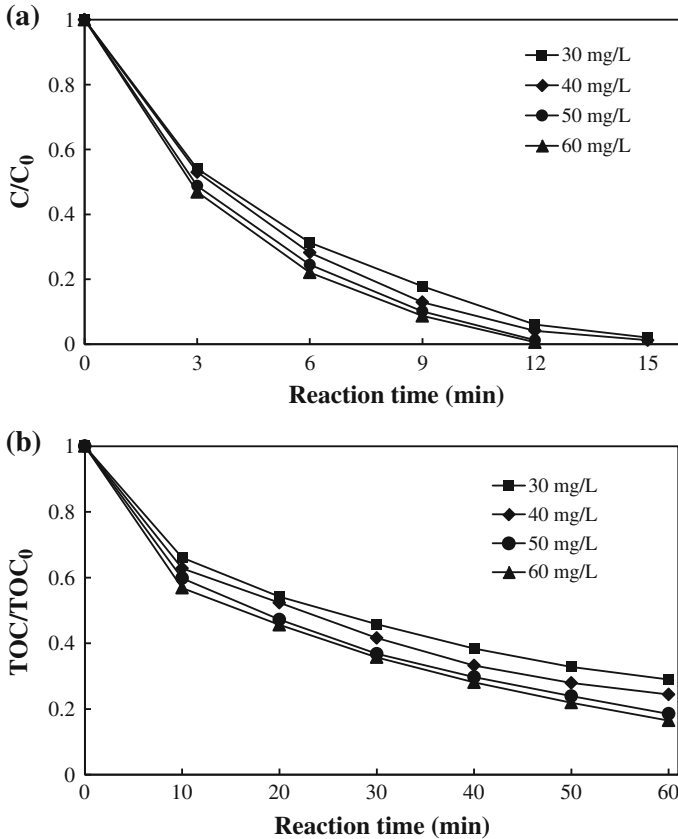


Fig. 7 Effect of amount of catalyst on the **a** degradation and **b** mineralization of CNB by the $O_3/US/TiO_2$ process. Experimental conditions: $C_0 = 40$ mg/L, pH = 9, O_3 concentration = 5.8 mg/L, and US power = 400 W

experiments on the degradation of 4-CNB were performed by coupled sonocatalytic ozonation.

Effect of operating conditions on sonocatalytic ozonation, and reusability of the nanocatalyst

The effects of the main operating conditions, for example initial 4-CNB and ozone concentrations, pH, US power, and amount of catalyst, on the degradation and mineralization of 4-CNB were studied. Degradation of 4-CNB was reduced by increasing its concentration (Fig. 3a) because the same amounts of oxidizing species generated under identical experimental conditions had to degrade more 4-CNB and its degradation products [29]. Degradation of 4-CNB by indirect attack of hydroxyl radicals under basic conditions seemed to be more efficient than direct electrophilic attack under acidic conditions under otherwise similar operating conditions

Table 2 Effect of operating conditions on the apparent pseudo-first-order rate constants for degradation and mineralization of 4-CNB by use of the O₃/US/TiO₂ process

Operating conditions and amounts ^a	Degradation rate constant (min ⁻¹)	Correlation coefficient (R ²)	Mineralization rate constant (min ⁻¹)	Correlation coefficient (R ²)
4-CNB concentration (mg/L)				
20	0.431	0.940	0.030	0.959
40	0.347	0.931	0.026	0.977
60	0.153	0.995	0.019	0.978
80	0.083	0.974	0.017	0.993
pH				
3	0.208	0.995	0.016	0.928
6	0.304	0.970	0.019	0.942
9	0.347	0.931	0.026	0.977
O ₃ concentration (mg/L)				
1.4	0.128	0.989	0.018	0.970
3.6	0.207	0.992	0.022	0.979
5.8	0.347	0.931	0.026	0.977
US power (W)				
80	0.108	0.981	0.012	0.947
240	0.152	0.990	0.017	0.940
400	0.347	0.931	0.026	0.977
Amount of TiO ₂ (mg/L)				
30	0.254	0.972	0.019	0.962
40	0.291	0.976	0.022	0.968
50	0.347	0.929	0.026	0.977
60	0.398	0.904	0.027	0.977

^a Other operating conditions: [4-CNB]₀ = 40 mg/L, pH = 9, O₃ concentration = 5.8 mg/L, US power = 400 W, and amount of TiO₂ = 50 mg/L

(Fig. 4a), consistent with other research [30]. pH 9 was therefore chosen to perform the remaining experiments. Increasing the O₃ concentration (Fig. 5a) and US power (Fig. 6a), increased the degradation of 4-CNB, owing to the production of more ROS, especially hydroxyl radicals, as explained above [6, 17]. The effect of the amount of TiO₂ is shown in Fig. 7a; 50 mg/L was selected as the optimum amount; for larger amounts, screening of the effect of the ultrasonic waves by TiO₂ particles prevented the solution from receiving the same amount of dissipated energy and reduced the amount of degradation [6].

The same effects of operating conditions were obtained for mineralization of 4-CNB (Figs. 2b, 3b, 4b, 5b, 6b, 7b). All the apparent rate constants for degradation and mineralization of 4-CNB (Table 2) were determined by assuming pseudo-first-order kinetics (Eq. 15). In general, for all the AOPs, the rate of mineralization was

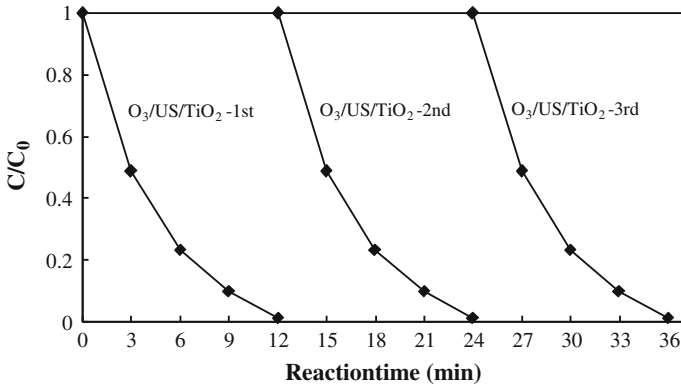


Fig. 8 Reusability profiles obtained during successive runs. Experimental conditions: $C_0 = 40$ mg/L, pH = 9, O_3 concentration = 5.8 mg/L, US power = 400 W, and amount of $TiO_2 = 50$ mg/L

less than the rate of degradation under the same operating conditions, because of the need to oxidize the intermediates produced to water, carbon dioxide, and inorganic salts [28].

The activity of a catalyst in successive applications is of practical significance. Three replicate degradations of 4-CNB were conducted under the optimum conditions. After each run, the catalyst was recovered and dried for the next experiment. As is apparent from Fig. 8, the amount of degradation was the same after three repeated runs. This confirmed not only the reusability and stability of the catalyst, but also the reliability of the results for the $O_3/US/TiO_2$ process.

Conclusion

In this research study, sonocatalytic ozonation for degradation of 4-CNB, as model persistent organic pollutant, was compared with US, US/TiO_2 , O_3 , O_3/TiO_2 , and US/O_3 and selected as the most effective. Moreover, all processes obeyed pseudo-first-order kinetics. The effect of the main operating conditions—initial 4-CNB and ozone concentrations, initial pH, US power, and amount of catalyst—on the degradation of 4-CNB was then studied in the coupled $O_3/US/TiO_2$ process, for which a substantial synergistic effect was observed compared with the O_3 and US/TiO_2 processes individually. The efficiency of degradation was reduced by increasing the 4-CNB concentration; the opposite trend was observed for O_3 concentration and ultrasonic power; pH 9 and 50 mg/L TiO_2 were chosen as optimum. Finally, total organic carbon was monitored during the processes to study the mineralization of 4-CNB; similar results were obtained except rates of mineralization were lower than rates of degradation under the same operating conditions.

Acknowledgments The authors would like to thank Tabriz Branch, Islamic Azad University for the financial support of this research, which is based on a research project contract.

References

1. M. Ye, Z. Chen, X. Liu, Y. Ben, J. Shen, J. Hazard. Mater. **167**, 1021–1027 (2009)
2. J.M. Shen, Z. Chen, Z. Xu, X. Li, B. Xu, F. Qi, J. Hazard. Mater. **152**, 1325–1331 (2008)
3. Z. Guo, S. Zheng, Z. Zheng, F. Jiang, W. Hu, L. Ni, Water Res. **39**, 1174–1182 (2005)
4. N. Getoff, Res. Chem. Intermed. **27**, 343–358 (2001)
5. M.A. Behnajady, N. Modirshahla, M. Shokri, B. Vahid, Ultrason. Sonochem. **15**, 1009–1014 (2008)
6. Y.L. Pang, A.Z. Abdullah, S. Bhatia, Desalination **277**, 1–14 (2011)
7. P. Pichat, L. Cermenati, A. Albini, D. Mas, H. Delprat, C. Guillard, Res. Chem. Intermed. **26**, 161–170 (2000)
8. M.N. Chong, B. Jin, C.W. Chow, C. Saint, Water Res. **44**, 2997–3027 (2010)
9. T.J. Mason, J.P. Lorimer, *Applied Sonochemistry: The Uses of Power Ultrasound in Chemistry and Processing*, 1st edn. (Wiley-VCH, Weinheim, 2002)
10. M.A. Behnajady, N. Modirshahla, M. Shokri, B. Vahid, Glob. Nest J. **10**, 8–15 (2008)
11. M. Kubo, K. Matsuoka, A. Takahashi, N. Shibasaki-Kitakawa, T. Yonemoto, Ultrason. Sonochem. **12**, 263–269 (2005)
12. A. Mahyar, M.A. Behnajady, N. Modirshahla, Photochem. Photobiol. **87**, 795–801 (2011)
13. M. Anpo, Pure Appl. Chem. **72**, 1265–1270 (2000)
14. E. Selli, Phys. Chem. Chem. Phys. **4**, 6123–6128 (2002)
15. T. Mousanejad, M. Khosravi, S. Tabatabaie, A.R. Khataee, K. Zare, Res. Chem. Intermed. **40**, 711–722 (2014)
16. Z. He, S. Song, M. Xia, J. Qiu, H. Ying, B. Lü, J. Chen, Chemosphere **69**, 191–199 (2007)
17. Y. Yang, J. Ma, Q. Qin, X. Zhai, J. Molecul. Catal. A **267**, 41–48 (2007)
18. C.D. Vecitis, T. Lesko, A.J. Colussi, M.R. Hoffmann, J. Phys. Chem. **114**, 4968–4980 (2010)
19. X. Xu, H. Shi, D. Wang, J. Zhejiang Univ. Sci. B **6**, 553–558 (2005)
20. K. Thamaphat, P. Limsuwan, B. Ngotawornchai, J. Kasetsart, Nat. Sci. **42**, 357–361 (2008)
21. B. Vahid, A.R. Khataee, Electrochim. Acta **88**, 614–620 (2013)
22. N. Shimizu, C. Ogino, M.F. Dadjour, T. Murata, Ultrason. Sonochem. **14**, 184–190 (2007)
23. J. Wang, Y. Jiang, Z. Zhang, X. Zhang, T. Ma, G. Zhang, Y. Li, Ultrason. Sonochem. **14**, 545–551 (2007)
24. F.J. Beltrán, F.J. Rivas, O. Gimeno, J. Chem. Technol. Biotechnol. **80**, 973–984 (2005)
25. M.H. Priya, G. Madras, Ind. Eng. Chem. Res. **45**, 913–921 (2006)
26. M.H. Priya, G. Madras, J. Photochem. Photobiol., A **179**, 256–262 (2006)
27. A.R. Khataee, A. Akbarpour, B. Vahid, J. Taiwan Inst. Chem. E **45**, 930–936 (2013)
28. K. Rajeshwar, M. Osugi, W. Chanmanee, C. Chenthamarakshan, M. Zononi, P. Kajitvichyanukul, R. Krishnan-Ayer, J. Photochem. Photobiol., C **9**, 171–192 (2008)
29. C.H. Chiou, C.Y. Wu, R.S. Juang, Sep. Purif. Technol. **62**, 559–564 (2008)
30. A. Rodríguez, R. Rosal, J. Perdigón-Melón, M. Mezcua, A. Agüera, M. Hernando, E. García-Calvo, Hdb. Environ. Chem. **5**, 127–175 (2008)